



ORIGINAL ARTICLE

Neurodegeneration caused by Trimethyltin via inhibition of Tropomyosin Receptor Kinase A/B and Phosphoinositide-3-Kinase/Protein kinase B Signaling pathway

Tran Phi Hoang Yen^{a1}, Nguyen Ngoc Khoi^a, Duong Phuoc An^a, Nguyen Thi Thu Van^a

^a University of Medicine and Pharmacy of Ho Chi Minh City, Department of Pharmacy
41 Dinh Tien Hoang street, 1st district, Ho Chi Minh City, Viet Nam.

¹Corresponding author e-mail address: tranyen73@gmail.com

ABSTRACT

We recently reported that trimethyltin (TMT, 2.4 mg/kg, i.p) can trigger neuronal damage by inhibiting Tropomyosin receptor kinase A/B (TrkA/B receptor) following by phosphoinositide 3-kinase (PI3K)/protein kinase B (Akt) signaling pathway. We examined hippocampal changes in TrkA/B phosphorylation on Tyr490/Tyr516 of TMT-treated mice in a time-dependent manner. Phospho-PI3K (Tyr508), phospho-3-phosphoinositide-dependent protein kinase 1 (PDK1) (Ser241) and phospho-Akt (Ser473) were changed following by TMT injury (from 3 hours until 7 days after injury). Pretreatment with 7,8-dihydroxyflavone (7,8-DHF), a specific TrkB receptor agonist, significantly attenuated the TMT-caused inhibition of phospho-TrkA/B, thereby increased in expressions of phospho-PI3K, phospho-PDK1 and phospho-Akt in TMT-treated mice, simultaneously 7,8-DHF showed a neuroprotective effect in observation of nuclear chromatic clumping by Cresyl violet and Terminal deoxynucleotidyl transferase-mediated dUTP nick-end labeling (TUNEL-) staining in the dentate gyrus (DG) of the TMT-injected mice. This finding suggests that inhibition of TrkA/B receptor following by PI3K/Akt cascade may play a role in the molecular mechanism of TMT-induced neurodegeneration in mice.

Key-words: trimethyltin, neurodegeneration, TrkA/B receptor, PI3K/Akt pathway, mice

Received 20/11/2013 Accepted 27/12/2013

©2014 AELS, INDIA

Abbreviations: Akt, protein kinase B; BDNF, Brain-derived neurotrophic factor; DG, dentate gyrus; I.P, intraperitoneal; PDK1, 3-phosphoinositide-dependent protein kinase 1; PI3K, phosphoinositide 3-kinase; TMT, trimethyltin; TrkA/B, Tropomyosin receptor kinase A/B; TUNEL, Terminal deoxynucleotidyl transferase-mediated dUTP nick-end labeling; 7,8-DHF, 7,8-dihydroxyflavone.

Running title: Trimethyltin neurotoxicity via TrkA/B and PI3K/Akt pathway

INTRODUCTION

Selective neurodegeneration caused by trimethyltin (TMT), an organotin compound, was demonstrated in the hippocampal dentate gyrus (DG) of mice [8,9,11,13]. Until now, the molecular mechanisms underlying neuronal damage by TMT intoxication have remained unclear. We reported previously the effect of TMT on the Phosphoinositide 3-kinase (PI3K)/ Protein kinase B (Akt) signaling pathway in a study designed to investigate the role of the interleukin-6 (IL-6) gene against TMT-induced neurotoxicity in IL-6 knock-out mice [12]. It was demonstrated that phospho-Akt (at Thr308) was decreased in the hippocampus of mice after TMT exposure, followed by increases in the phosphorylation of Bad and the subsequent expression of Bcl-xL and Bcl-2. It was known that tropomyosin receptor kinase B (TrkB receptor), a high affinity brain-derived neurotrophic factor (BDNF) receptor, drives signaling through the PI3K and Ras pathways. As such, TrkB mediates the multiple effects of these neurotrophic factors, which includes neuronal differentiation and survival [2,6]. To expand on our previous study and to better understand the regulation of the PI3K/Akt signaling pathway after TMT treatment as a function of time, we here focused on changes in phospho-TrkA/B and its downstream PI3K/Akt cascade from 3 hours to 7 days after TMT administration. In the 7,8-dihydroxyflavone (7,8-DHF) study, presence of 7,8-DHF, a selective TrkB receptor agonist, enhanced expressions of phospho-TrkA/B, phospho-PI3K, phospho-PDK1 and phospho-Akt along with a simultaneous neurodegeneration in the hippocampus, which was detected using Cresyl violet and TUNEL-staining.

MATERIALS AND METHODS

Animals

All animals were treated in strict accordance with the National Institutes of Health (NIH) Guide for the Humane Care and Use of Laboratory Animals (NIH Publication No. 85-23, 1985; www.dels.nas.edu/ila). Swiss Albino mice were supplied by the Institute of Vaccines and Medical Biologicals at Nha Trang Town, Viet Nam. The male mice, weighing ~24-28g, were maintained on a 12:12 h light: dark cycle and were fed *ad libitum*. They were allowed to adapt to these conditions for 1 week before the experiment.

Drug treatment

Trimethyltin hydrochloride (TMT; Sigma-Aldrich) was dissolved in sterile saline immediately before use. For TMT experiments, mice received a single intraperitoneal injection of TMT (2.4 mg/kg) or saline. Mice were sacrificed at 3 h, 6 h, 12 h, 1 d, 2 d, 3 d and 7 d after TMT treatment for western blotting analysis to detect TrkA/B and PI3K/Akt signaling. For TrkB agonist experiments, 7,8-dihydroxyflavone (7,8-DHF; Sigma-Aldrich, St Louis, MO) was dissolved in phosphate-buffered saline (PBS) containing 17% dimethylsulfoxide (DMSO). Mice received a single intraperitoneal injection of 7,8-DHF (10 mg/kg) 30 min before they were injected with TMT. Mice were sacrificed at 2 d after TMT treatment for western blotting analysis to detect TrkA/B and PI3K/Akt signaling and neurodegenerative analysis using Cresyl violet staining and Terminal deoxynucleotidyl transferase-mediated dUTP nick-end labeling (TUNEL) staining.

Cresyl Violet-staining and neuron counts

Cresyl Violet-staining was performed to visualize neuronal cell death in the hippocampus caused by TMT. Nuclear clumping counts were conducted in dentate gyrus of hippocampus. Every sixth section (200 μ m separation distance) was evaluated with a 100 \times oil immersion objective on an Olympus microscope using a video camera and monitor [5].

Terminal deoxynucleotidyl transferase-mediated dUTP nick-end labeling (TUNEL) staining

TUNEL staining was performed using the FragEL DNA fragmentation detection kit (QIA33; Calbiochem, La Jolla, CA, USA) following by the manufacturer's protocol. Briefly, sections were permeabilized by incubation with 20 mg/ml proteinase K and then incubated with 3% hydrogen peroxide for blocking endogenous peroxidase activity. After immersion in the terminal deoxynucleotidyl transferase (TdT) equilibration buffer, sections were incubated with biotinylated deoxynucleotides and TdT enzyme. And then, sections were immersed in streptavidin-peroxidase complex. DAB was used as a chromogen. Counterstaining was done with methyl green provided in the kit. Digital images were acquired at 40 \times or 100 \times magnification using an Olympus microscope: OD 16592, Model: CX21, Olympus optical Co.,Ltd.

Western blotting

Western blotting was performed as described previously [12]. Hippocampi were dissected immediately after decapitation and frozen in liquid nitrogen. Hippocampal tissues were homogenized in lysis buffer, containing 200mM Tris-HCl (pH 6.8), 1% SDS, 5 mM ethylene glycol-bis(2-aminoethyl ether)-N,N,N',N'-tetraacetic acid, 5 mM EDTA, 10% glycerol, 1 \times phosphatase inhibitor cocktail I (Sigma-Aldrich) and 1 \times protease inhibitor cocktail (Sigma-Aldrich). The lysate was centrifuged at 12,000 $\times g$ for 30 min and the supernatant fraction was subjected to Western blotting. Proteins (20-50 μ g/lane) were separated by 8 or 10% sodium dodecyl sulfate (SDS)-polyacrylamide gel electrophoresis (PAGE) and transferred onto polyvinylidene difluoride (PVDF) membranes. After transfer, the membranes were preincubated with 5% nonfat milk for 30 min and incubated overnight at 4 $^{\circ}$ C with primary antibodies against β -actin (8H10D10) mouse mAb (1:10000, Sigma-R1281), anti-TrkB (Ab-705) antibody (1:1000, Sigma-SAB4300702), anti-phospho Trk A/B (Tyr490/Tyr516) (1:500, Cellsignaling, C50F3), anti-PDK1 antibody (1:1000, HPA027376, Sigma), anti-phospho-PDK1 (Ser241) (1:500, SAB4504514, Sigma), anti-PI3-K p85 antibody (1:1000, Sigma-HPA001216), anti-phospho PI3-K p85a (Tyr508) (1:500, Sigma- S8563), anti-Akt antibody (1:1000, Sigma-HPA002891) and anti-phospho Akt (Ser473) (1:500, Sigma-P4112). The membranes were then incubated with horseradish peroxidase-conjugated secondary anti-rabbit IgG (1:1000, Sigma-PM0100) or anti-mouse IgG (1:1000, Sigma-M6898) for 2 h. Subsequent visualization was performed using an enhanced chemiluminescence system (ECL Plus; GE Healthcare). Relative intensities of the bands were quantified by PhotoCapt MW (version 10.01 for Windows; Vilber Lourmat, Marne la Vallée, France).

Statistics

The data were analyzed using a one-way ANOVA. Post hoc Fischer's PLSD test followed. *P* values of less than 0.05 were deemed to indicate statistical significance.

RESULTS AND DISCUSSION

It was accepted that TMT was evenly distributed across the cerebellum, medulla-pons, hypothalamus, hippocampus, and striatum following TMT exposure [3,7] and caused neuronal degeneration in hippocampus of mice. Our study was performed to take a part in looking for a reasonable molecular

mechanism by which TMT causes neurodegeneration. Until now, changes in TrkA/B in the dentate gyrus (DG) of hippocampus of TMT-exposed mice were not published. One study on rats indicated that decrease in TrkB mRNA was seen in the CA3 pyramidal cell layer at 3 days after TMT treatment [1]. This result is consistent with our data from current study showing that TMT inhibited activation of TrkA/B receptor, as detected by western blot analysis. Although no changes in the TrkB in the mouse hippocampal DG from 3 hours to 7 days following a single dose of TMT were detected, dramatic decreases in p-TrkA/B were detected from 6 hours to 7 days post-TMT administration, with the largest decrease occurring at 2 days (data are shown in figure 1A: density of p-TrkA/B expression of 3 h post-TMT group/ β -actin: 0.637 ± 0.047 , $P = 0.62$; 6 h post-TMT 0.417 ± 0.089 , $P = 9 \times 10^{-4}$; 12 h post-TMT 0.328 ± 0.086 , $P = 2.09 \times 10^{-5}$; 1 d post-TMT 0.009 ± 0.002 , $P = 1.57 \times 10^{-11}$; 2 d post-TMT 0.006 ± 0.020 , $P = 1.39 \times 10^{-11}$; 3 d post-TMT 0.183 ± 0.017 , $P = 3.13 \times 10^{-8}$; 7 d post-TMT 0.155 ± 0.013 , $P = 8.84 \times 10^{-9}$, compared with control group). Interestingly, the expression of p-TrkA/B was almost disappeared at 2 d post-TMT, correlated with neuronal degeneration data in the dentate gyrus of hippocampus assessed by Cresyl violet and TUNEL-staining. This suggests that TMT may directly or indirectly affect phosphorylation of TrkA/B, leading to subsequent changes in its downstream molecular signaling, inducing neuronal toxicity. Moreover, to address whether TMT has an impact on p-PI3K in time dependently, western blot analysis for PI3K and constitutive activation of PI3K were performed. We found that p-PI3K was decreased in the hippocampus of TMT-treated mice, whereas PI3K total changes were not detected. These changes were evident early after TMT treatment (data are shown in figure 1B: density of protein expression of 3 h post-TMT group/ β -actin: 0.598 ± 0.039 , $P = 1.34 \times 10^{-10}$; 6 h post-TMT 0.187 ± 0.019 , $P = 1.05 \times 10^{-21}$; 12 h post-TMT 0.086 ± 0.014 , $P = 1.03 \times 10^{-23}$; 1 d post-TMT 0.190 ± 0.023 , $P = 1.21 \times 10^{-21}$; 2 d post-TMT 0.199 ± 0.022 , $P = 1.93 \times 10^{-21}$; 3 d post-TMT 0.003 ± 0.001 , $P = 3.12 \times 10^{-25}$; 7 d post-TMT 0.000 ± 0.000 , $P = 2.81 \times 10^{-25}$, compared with saline group). Following the time-dependent decrease in p-PI3K in TMT-treated animals, we examined whether there were changes in PDK1 and p-PDK1 to address whether TMT neurotoxicity had any impact on the PI3K/Akt signaling pathway. In the early term course of TMT injury, no change of p-PDK1 was detected (data are shown in figure 1C: $P = 0.057$ and $P = 0.656$ for 3 h and 6 h-post TMT vs. saline, respectively). Significant increases in p-PDK1 were noted in 12 h and 1 d post-TMT injury (data are shown in figure 1C: density of protein expressions of 12 h post-TMT group/ β -actin: 2.251 ± 0.058 , $P = 1.04 \times 10^{-6}$ and 1 d post-TMT 2.063 ± 0.062 , $P = 3.26 \times 10^{-5}$, compared with saline group). Downregulation of p-PDK1 in the hippocampus was observed from 2 d to 7 d post-TMT administration (data are shown in Figure 1C: density of protein expression of 2 d post-TMT group/ β -actin: 0.900 ± 0.052 , $P = 4.85 \times 10^{-11}$; 3 d post-TMT 1.048 ± 0.039 , $P = 9.3 \times 10^{-10}$, and 7 d post-TMT 0.017 ± 0.006 , $P = 1.13 \times 10^{-19}$, compared with saline group). Phospho-Akt decreased in the hippocampus from 6 h until 7 d of TMT treatment (data are shown in figure 1D: density of p-Akt expressions of 3 h post-TMT group/ β -actin: 1.091 ± 0.053 , $P = 0.008$; 6 h post-TMT 0.952 ± 0.050 , $P = 0.783$; 12 h post-TMT 0.842 ± 0.041 , $P = 0.125$; 1 d post-TMT 0.252 ± 0.017 , $P = 2.87 \times 10^{-14}$; 2 d post-TMT 0.524 ± 0.035 , $P = 5.5 \times 10^{-9}$; 3 d post-TMT 1.010 ± 0.050 , $P = 0.075$; 7 d post-TMT 0.787 ± 0.040 , $P = 0.004$, compared with saline group). Trk receptors affect neuronal survival and differentiation through several signal cascades, such as cell survival PI3K/Akt cascade [4]. Once phosphorylated, Trk receptors affect neuronal survival and differentiation through several signal cascades, such as the stimulation of P13 heterodimers, and cause the activation of kinases PDK-1 and Akt [10]. To investigate whether neurodegeneration induced by TMT in mice model was due to inhibition of TrkB receptor, 7,8-DHF, a selective agonist receptor of TrkB was administrated to assess changes in p-TrkA/B, p-PI3K, p-PDK1 and p-Akt in mouse hippocampi at 2 days after TMT treatment. Two days after TMT treatment, changes in p-TrkA/B and others indexes were more pronounced, so this time point was chosen in 7,8-DHF study. Pretreatment with 7,8-DHF 30 min before TMT attenuated inhibition of p-TrkA/B, p-PI3K, p-PDK1 and p-Akt expressions. Data are shown in figure 2A: density of p-TrkA/B expression of 7,8-DHF + TMT group/ β -actin: 0.413 ± 0.031 , $P = 1 \times 10^{-4}$, compared with TMT group. Data are shown in figure 2B: density of p-PI3K expression of 7,8-DHF + TMT group/ β -actin: 0.452 ± 0.022 , $P = 3 \times 10^{-4}$, compared with TMT group. 7,8-DHF was also showed a neuroprotective effect in TMT mouse model using Cresyl violet- (figure 2C) and TUNEL-staining (figure 2D). Two days after TMT administration, neurodegeneration and neuronal loss were strong detected in the DG of mouse's hippocampi (figure 2F-b). TUNEL-staining was applied for detection the presence of fragmented DNA in hippocampal samples. Results revealed that very few TUNEL-positive were observed in the dentate gyrus of hippocampus of saline-treated mice, but after TMT treatment, the number of TUNEL-positive cells was significantly increased ($P < 0.001$). Simultaneously, a very few of nuclear chromatin clumping was detected in saline-treated mice, while this signal dramatically increased at 2 d after TMT treatment ($P < 0.001$). 7,8-DHF-treated mice showed a significant attenuates neuronal toxication induced by TMT as showed by Cresyl violet- and TUNEL-staining data (data are shown in Figure 2E and 2F). In conclusion, this study was to elucidate the molecular mechanism by which TMT-mediated neuronal degeneration occurs. Our research suggests that the inhibition of activated-TrkA/B

receptor in mice caused by TMT intoxication is an important initial step toward neurodegenerative process. That was PI3K/Akt signaling pathway, including decreases in the expressions of p-PI3K, p-PDK1 and p-Akt in the dentate gyrus (DG) of the hippocampus of mice. Although we could not demonstrate that TMT causes neurodegeneration via binding to TrkB receptor, then inhibits this receptor, at least, it takes part in demonstrating that TMT may produce neurodegenerative effect via inhibiting TrkA/B receptor and its downstream, PI3K/Akt cell survival signaling pathway.

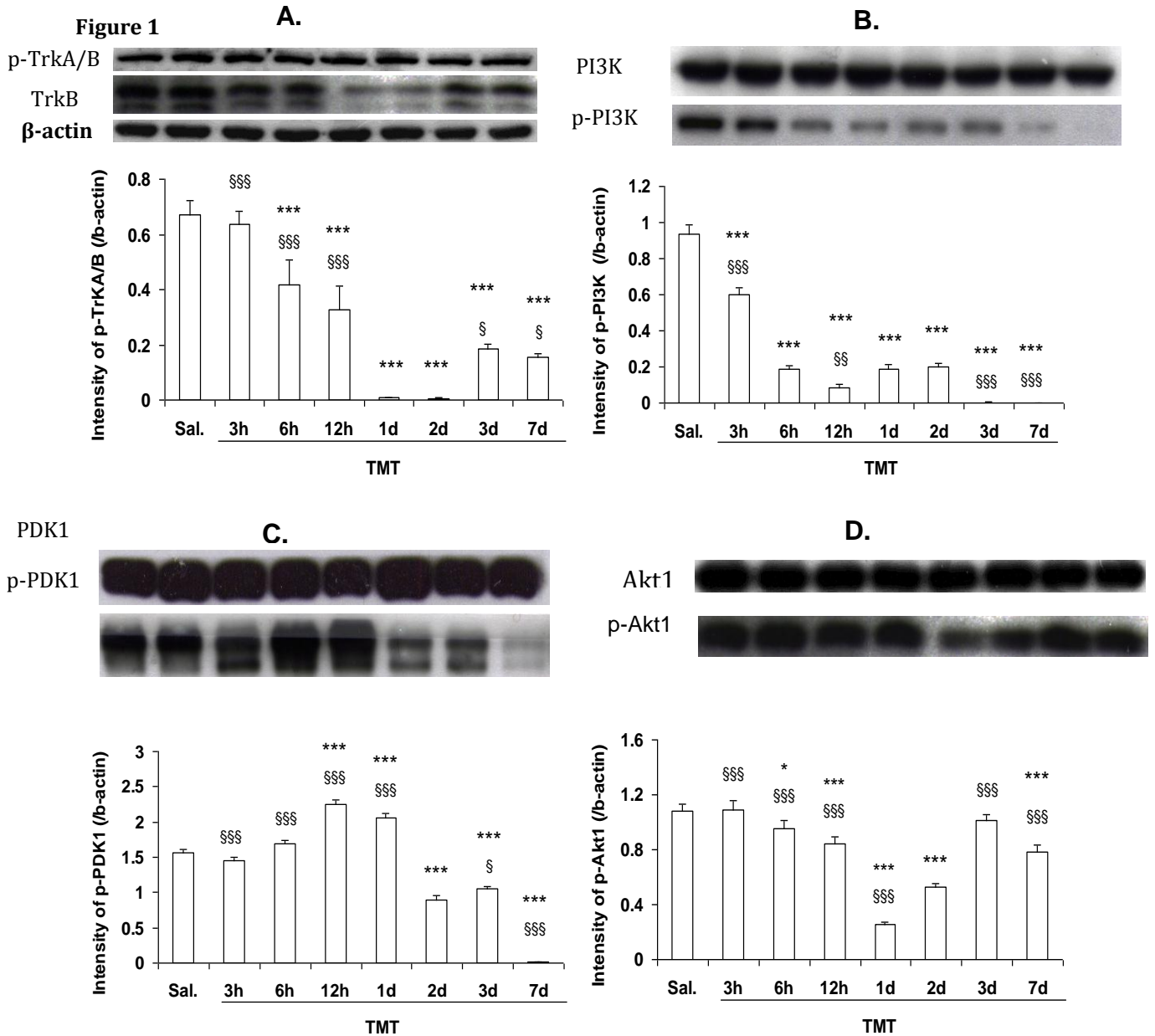


Figure 1. Time-dependent hippocampal changes in TrkB receptors, phospho-TrkA/B receptors (Figure 1A); PI3K and phospho-PI3K (Figure 1B); PDK1 and phospho-PDK1 (Figure 1C); and Akt and phospho-Akt (Figure 1D) of TMT-treated mice. Reductions in phospho-TrkA/B but not total TrkB were detected 3 h, 6 h, 12 h, 2 d, 3 d, and 7 d after TMT treatment. Also, reductions in phospho-PI3K, phospho-PDK1, and phospho-Akt were detected in time dependently. Each value is the mean±SEM of six mice. * $P < 0.05$, and *** $P < 0.001$ vs corresponding saline-treated mice; § $P < 0.05$, §§ $P < 0.01$, SSS $P < 0.001$ vs corresponding 2 d after TMT-treated mice (One-way ANOVA followed by Fisher's PLSD test).

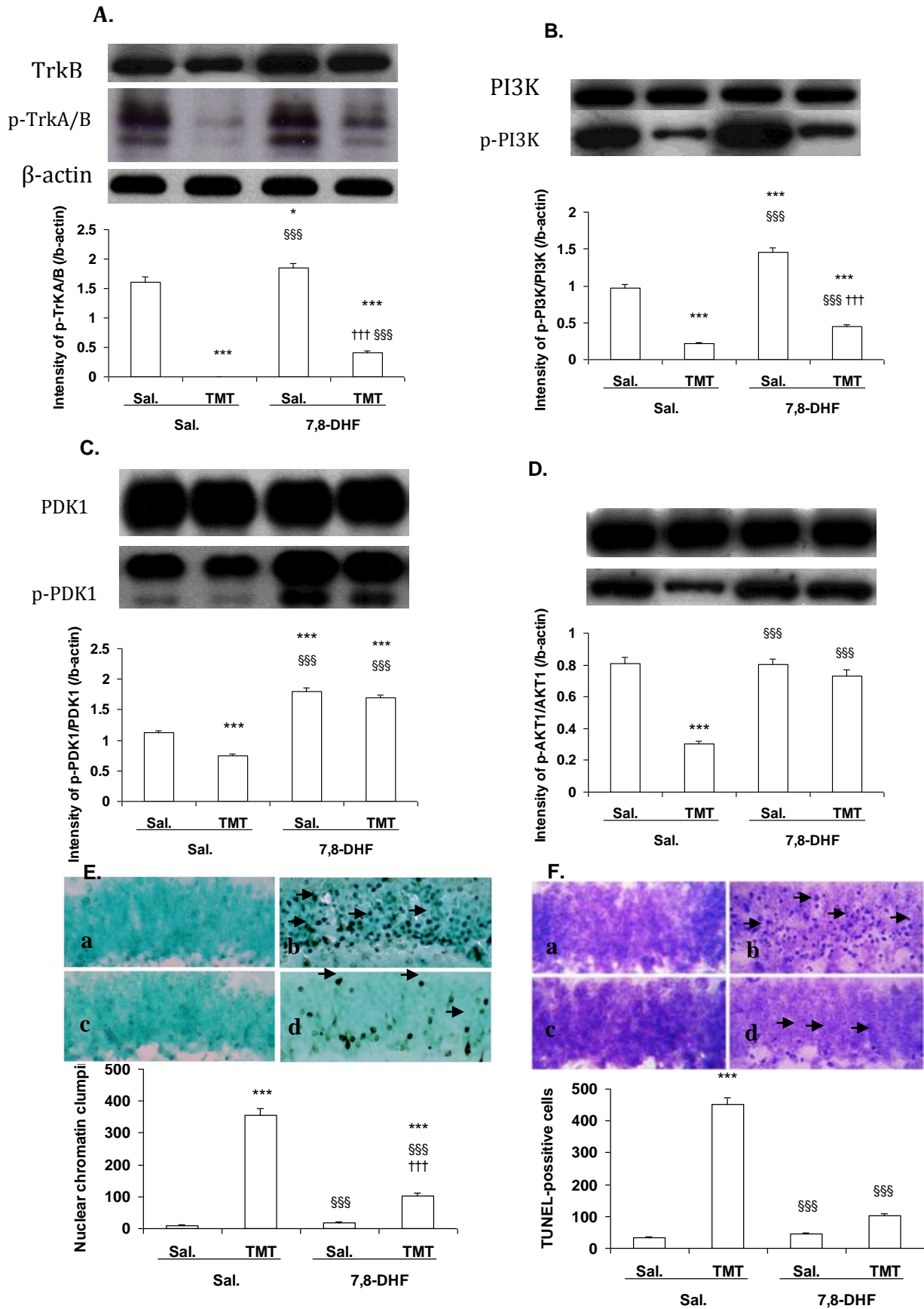


Figure 2. Effects of 7,8-DHF on TMT-induced changes in TrkB receptors, phospho-TrkA/B receptors (Figure 2A); PI3K and phospho-PI3K (Figure 2B); PDK1 and phospho-PDK1 (Figure 2C); Akt and phospho-Akt (Figure 2D) expressions. In the presence of 7,8-DHF, TMT-induced TUNEL-positive cells (Figure 2E - a, saline; b, TMT; c, 7,8-DHF 10 mg/kg; d, 7,8-DHF 10 mg/kg +TMT) and nuclear chromatin clumping counts assessed by Cresyl violet staining (Figure 2F - a, saline; b, TMT; c, 7,8-DHF 10 mg/kg; d, 7,8-DHF 10 mg/kg +TMT) were observed. Each scale bar = 100

µm. Each value is the mean±S.E.M of six animals. * $P<0.05$, *** $P<0.001$ vs corresponding saline-treated mice; §§§ $P<0.001$ vs corresponding 2 d after TMT-treated mice; +++ $P<0.001$ vs corresponding 7,8-DHF-treated mice (one-way ANOVA followed by Fisher's PLSD test).

ACKNOWLEDGEMENTS

This study was mainly supported by a grant from the National Foundation For Sciences & Technology Development (NAFOSTED) in Viet Nam (Code of study: 106.99-2010.76)

REFERENCES

1. Andersson, H., Wetmore, C., Lindqvist, E., Luthman, J., Olson, L. (1997). Trimethyltin exposure in the rat induces delayed changes in brain-derived neurotrophic factor, fos and heat shock protein 70. *Neurotoxicology*, 18:147-59.
2. Calella, A., Nerlov, C., Lopez, R., Sciarretta, C., Halbach, O., Bereshchenko, O., and Minichiello, L. (2007). Neurotrophin/Trk receptor signaling mediates C/EBP α , - β and NeuroD recruitment to immediate-early gene promoters in neuronal cells and requires C/EBPs to induce immediate-early gene transcription. *Neural Dev*, 2:4
3. Cook, L.L., Stine, K.E., Reiter, L.W. (1984). Tin distribution in adult rat tissues after exposure to trimethyltin and triethyltin. *Toxicol Appl Pharmacol*, 76:344-8.
4. Huang, E.J., Reichardt, L.F. (2003). Trk receptors: roles in neuronal signal transduction. *Annu. Rev. Biochem*, 72:609–642.
5. Kim, H.C., Bing, G., Jhoo, W.K., Kim, W.K., Shin, E.J., Park, E.S., Choi, Y.S., Lee, D.W., Shin, C.Y., Ryu, J.R., Ko, K.H. (2002). Oxidative damage causes formation of lipofuscin-like substances in the hippocampus of the senescence-accelerated mouse after kainate treatment. *Behav Brain Res*, 131:211–220.
6. Minichiello, L., Korte, M., Wolfert, D., Kühn, R., Unsicker, K., Cestari, V., Rossi-Arnaud, C., Lipp, H., Bonhoeffer, T., and Klein, R. (1999). Essential Role for TrkB Receptors in Hippocampus-Mediated Learning. *Neuron*, 24:401-414.
7. Moser, V.C., McGee, J.K., Ehman, K.D. (2009). Concentration and persistence of tin in rat brain and blood following dibutyltin exposure during development. *J Toxicol Environ Health A*, 72:47-52.
8. Noriko, H., Shozo, O., Takashi, S., Satoshi, M., and Shoei, F. (2010). Royal Jelly Facilitates Restoration of the Cognitive Ability in Trimethyltin-Intoxicated Mice. *J. Cell. Physiol*, 224:710–721.
9. Ogita, K., Nishiyama, N., Sugiyama, C., Higuchi, K., Yoneyama, M., Yoneda, Y. (2005). Regeneration of granule neurons after lesioning of hippocampal dentate gyrus: evaluation using adult mice treated with trimethyltin chloride as a model. *J. Neurosci. Res*, 82:609–621.
10. Segal, R.A. (2003). "Selectivity in Neurotrophin Signalling: Theme and Variations". *Annual Review of Neuroscience*, 26:299–330.
11. Shin, E.J., Suh, S.K., Lim, Y.K., Jhoo, W.K., Hjelle, O.P., Ottersen, O.P., Shin, C.Y., Ko, K.H., Kim, W.K., Kim, D.S., Chun, W., Ali, S., Kim, H.C. (2005). Ascorbate attenuates trimethyltin-induced oxidative burden and neuronal degeneration in the rat hippocampus by maintaining glutathione homeostasis. *Neuroscience*, 133:715–727.
12. Tran, H.Y., Shin, E.J., Saito, K., Nguyen, X.K., Chung, Y.H., Jeong, J.H., Bach, J.H., Park, D.H., Yamada, K., Nabeshima, T., Yoneda, Y., Kim, H.C. (2012). Protective potential of IL-6 against trimethyltin-induced neurotoxicity in vivo. *Free Radic Biol Med*. 2012 Apr 1;52(7):1159-74. doi: 10.1016/j.freeradbiomed.2011.12.008
13. Yoneyama, M., Nishiyama, N., Shuto, M., Sugiyama, C., Kawada, K., Seko, K., Nagashima, R., Ogita, K. (2008). In vivo depletion of endogenous glutathione facilitates trimethyltin-induced neuronal damage in the dentate gyrus of mice by enhancing oxidative stress. *Neurochem. Int*, 52:761–769.

How to cite this article

Tran P H Y, Nguyen N K, Duong P A, Nguyen T T V. Neurodegeneration caused by Trimethyltin via inhibition of Tropomyosin Receptor Kinase A/B and Phosphoinositide-3-Kinase/Protein kinase B Signaling pathway. *Bull. Env. Pharmacol. Life Sci*. 3 (2) 2014: 269-274